

Nanoindentation Tip mechanics ascribing bluntness during fracture of thin coatings

A.S. Bhattacharyya

Department of Metallurgical and Materials Engineering, Central University of Jharkhand, Ranchi 835205, India¹

[§]Corresponding author: 2006asb@gmail.com, arnab.bhattacharya@cuja.ac.in

ABSTRACT

Nanoindentation is used for the determination of mechanical properties of thin-coatings comprising a mixture of hard phases. The load-depth plots represent minor fracture (energy \sim pJ) taken place due to assorted crystallization on the surface. The tip movement during the fracture is influenced by strain hardening due to brittle to ductile transformation and the amount of tip-bluntness as evident from the fractorial normal stiffness.

KEYWORDS: Nanoindentation, thin coatings, strain-hardening, tip-bluntness, fractorial normal stiffness

INTRODUCTION

The depth sensing nanoindentation has been efficient procedures for determining the mechanical properties of hard coatings for quite some time. Because of their high precision, the variations in crystallinity caused by compositional or depositional characteristics are represented with clarity. The fracture features of the sample surface that have been subjected to loading are also related to compositional changes that cause phase changes [1- 4].

The location of the indentation can disclose important information about the surface properties of the material being studied. The load-depth charts change depending on the morphological region of the sample. The tip-sample interactions for indentations done on the grain, grain boundary, or triple junctions are reflected in the P-h plots, which when analyzed can provide us with significant information, especially for materials that rely on surface-based phenomena such as conduction, adhesion, wear, abrasion, and so on [5, 6]. The electron flow and even piezoelectricity have been discovered in certain nanocomposites such as Si-C-N, extending their application in sensors and nano/micro-electro-mechanical systems (N/MEMS) [7].

Failure mechanisms associated with nanoindentation, such as fracture, delamination, and chipping, are critical areas of research for quality inspection of technologically significant nanocomposite hard coatings based on Ti, B, Si, C, and N elements, as well as bioceramics such as hydroxyapatite, which are used in the fabrication of small scale high precision devices and bio-implants. The nanocomposite hard coatings comprising of

phases like SiC, Si₃N₄, CNx, TiC, TiN, TiB₂, cBN etc have applications in the fabrication of nano/micro-electro-mechanical systems (N/MEMS) based devices, interconnects as well as metallurgical protective coatings. Depending on the indenter form, the nature of the substrate, crystallographic qualities, pre-existing faults, internal micro-cracks, or pre-strain, the stress generated by the indenter can influence fracture morphology as well as interfacial fracture energy. [8-15]

MATERIAL & METHODS

The hard films which are in the form of nanocomposites SiCN and TiB₂ were deposited on silicon substrates by RF magnetron sputtering (HINDHIVAC, Bangalore) using a 2-inch sintered ceramic targets of SiC and TiB₂ with a supply of Argon, and nitrogen gas, details of which have been reported previously [15, 16]. The nanoindentation tests were performed by MTS Nanoindenter, USA having a 3-sided pyramidal Berkovich. Finite element Analysis (FEA) was performed using ABAQUS 6.13

RESULTS & DISCUSSIONS

The load-depth (P-h) plots corresponding to phenomenon involving fracture along with no fracture is shown in **Fig 1a**. The indentations were performed on the same film surface but with a gap of about **100 μm**. The difference aroused due to heterogeneous crystallization during the sputter-growth of the film as reported previously. The magnified version showing the step formation due to fracture is given in **Fig 1b**. As it can be seen an energy of **4 pJ** got dissipated due to the fracture process. The indenter tip during the event faces no resistance for penetrating 4nm until re-establishing contact with a hard phase underneath. A comparative plot showing the stiffness/Load vs depth showed a burst corresponding to the depth at which the contact is again reestablished. A discontinuity can be seen for the other case as there were no data available for the fractured region. The chances of fracture increases with the bluntness of the indenter tip, The increase in tip sharpness promotes plastic deformation. New dislocation created surrounding a crack in the plastic zone ($r_p = \Gamma_i / \pi H$) harden the material causing the burst as mentioned above [17]. The decrease in hardness of the region undergoing fracture as observed in **Fig 1d** corresponds to an increase in the plastic zone, ultimately causing an increase in interfacial toughness (Γ_i). The area under the curve as shown in the figure provides the factorial normal stiffness (S^n_f) of **25 N/m**.

The tip-movement of **12 nm** occurs in the whole event which consists of **4 nm** (h_f) of fracture and 8 nm of hardening caused by yielding (h_y). The ratio between the two ($h_y/h_f = 2$) can be considered as a parameter to indicate tip deformation that has taken place. The burst is also indicative of yielding to have re-initiated with a brittle to ductile contact transformation.

The results obtained were correlated with Finite Element Analysis showing the stress distribution beneath the indentation (**Fig 2a**). The plastic zone with radius r_p is formed in

the coating region beneath the indentation. The fracture gets manifested as cracks formed at the boundary of the plastic zone and extend into the hydrostatic elastic zone. Formation of emitted dislocations hardens the material. Tip bluntness causes enhanced projection of the plastic zone as spherical nature becomes dominant (**Fig 2b**).

CONCLUSIONS

The indentation process causing minor fracture involves tip movement caused by strain hardening. The tip shape change was estimated from the tip movement during the fracture process. A tip-bluntness factor of 2 and fractorial normal stiffness of 25 N/m were determined. The results obtained were correlated with Finite Element Modeling.

REFERENCE

1. Tomastik, J.; Ctvrtlik, R.; Ingr, T.; Manak, J.; Opletalova, A. Effect of Nitrogen Doping and Temperature on Mechanical Durability of Silicon Carbide Thin Films. *Sci. Rep.* **2018**, *8* (1). <https://doi.org/10.1038/s41598-018-28704-3>.
2. Lemoine, P.; Acheson, J.; McKillop, S.; van den Beucken, J. J.; Ward, J.; Boyd, A.; Meenan, B. J. Nanoindentation and Nano-Scratching of Hydroxyapatite Coatings for Resorbable Magnesium Alloy Bone Implant Applications. *J. Mech. Behav. Biomed. Mater.* **2022**, *133* (105306), 105306. <https://doi.org/10.1016/j.jmbbm.2022.105306>.
3. Nanda, G.; Chandran, N.; Babu Thiyagarajan, G.; Devasia, R.; Kumar, R. Mechanical Response and Thermal Expansion Characteristics of Spark Plasma Sintered Zr–La–B–C(O)-Based Precursor-Derived Ceramics. *Adv. Appl. Ceram. Struct. Funct. Bioceram.* **2022**, *121* (1), 31–38. <https://doi.org/10.1080/17436753.2022.2031666>.
4. Inoue, K.; Triawan, F.; Inaba, K.; Kishimoto, K.; Nishi, M.; Sekiya, M.; Sekido, K.; Saitoh, A. Evaluation of Interfacial Strength of Multilayer Thin Films Polymer by Nanoindentation Technique. *Mech. Eng. J.* **2019**, *6* (1), 18-00326-18-00326. <https://doi.org/10.1299/mej.18-00326>.
5. Liang, T.; Yu, Q.; Yin, Z.; Chen, S.; Liu, Y.; Yang, Y.; Lou, H.; Shen, B.; Zeng, Z.; Zeng, Q. Spatial Resolution Limit for Nanoindentation Mapping on Metallic Glasses. *Materials* **2022**, *15*, 6319. <https://doi.org/10.3390/ma15186319>
6. Sha, Z. D.; Wan, Q.; Pei, Q. X.; Quek, S. S.; Liu, Z. S.; Zhang, Y. W.; Shenoy, V. B. On the Failure Load and Mechanism of Polycrystalline Graphene by Nanoindentation. *Sci. Rep.* **2014**, *4* (1). <https://doi.org/10.1038/srep07437>.
7. Barrios, E.; Zhai, L. A Review of the Evolution of the Nanostructure of SiCN and SiOC Polymer Derived Ceramics and the Impact on Mechanical Properties. *Mol. Syst. Des. Eng.* **2020**, *5* (10), 1606–1641. <https://doi.org/10.1039/d0me00123f>.

8. Dash R, Bhattacharyya K, Bhattacharyya AS, Fracture associated with static and sliding indentation of multicomponent hard coatings on silicon substrates. *Fatigue & Frac of Eng Mater & Struc.* 2023; 46(4): 1641-1645.
9. Dash R, Bhattacharyya K, Kumar RP, Bhattacharyya AS. Intensified chipping during nanoindentation and the effect of friction on the interfacial fracture for thin films used in N/MEMS. *Eng Res Exp.* 2022 ;4(4):045012.
10. Ritambhara Dash, Kushal Bhattacharyya, Arnab S. Bhattacharyya; Stress distribution variations during nanoindentation failure of hard coatings on silicon substrates. *Nanotechnol. Precis. Eng.* 1 December 2023; 6 (4): 042001. <https://doi.org/10.1063/10.0022175>
11. R. Dash, Kushal Bhattacharyya, A.S. Bhattacharyya, Synergistic fractural features observed in Ti-B-Si-C hard coatings on enhancing the sharpness of nano indenters, *International Journal of Refractory Metals and Hard Materials*, 116, 2023,106373, <https://doi.org/10.1016/j.jirmhm.2023.106373>.
12. Ritambhara Dash, Kushal Bhattacharyya, Arnab S. Bhattacharyya, Film failure at earlier and later stages of nanoindentation in static and sliding modes, *Engineering Failure Analysis*, 150, 2023, 107353, <https://doi.org/10.1016/j.engfailanal.2023.107353>.
13. Bhattacharyya, Arnab; P. Kumar, Ramgiri; Acharya, Gaurav; Ranjan, Vivek *Current Smart Materials*, 2, 1, 2017 39-43(5) <https://doi.org/10.2174/2405465801666161130154515>
14. Bhattacharyya, A.S., Kumar, R.P., Priyadarshi, S. *et al.* Nanoindentation Stress–Strain for Fracture Analysis and Computational Modeling for Hardness and Modulus. *J. of Materi Eng and Perform* **27**, 2719–2726 (2018). <https://doi.org/10.1007/s11665-018-3289-7>
15. Ritambhara Dash, Arnab S. Bhattacharyya Crack growth based on indentation along substrate and nanocrystallites in titanium diboride thin films, 46, 7 2023, 2714-2719 <https://doi.org/10.1111/ffe.13986>
16. AS Bhattacharyya, SK Mishra, GC Das, S Mukherjee SiCN : Hot Properties *Eur. Coat. J* 3, 108-114
17. Ly, et al., Dynamical observations on the crack tip zone and stress corrosion of two dimensional MoS₂, *Nat. Commun.* 8 (2017) 14116

FIGURES

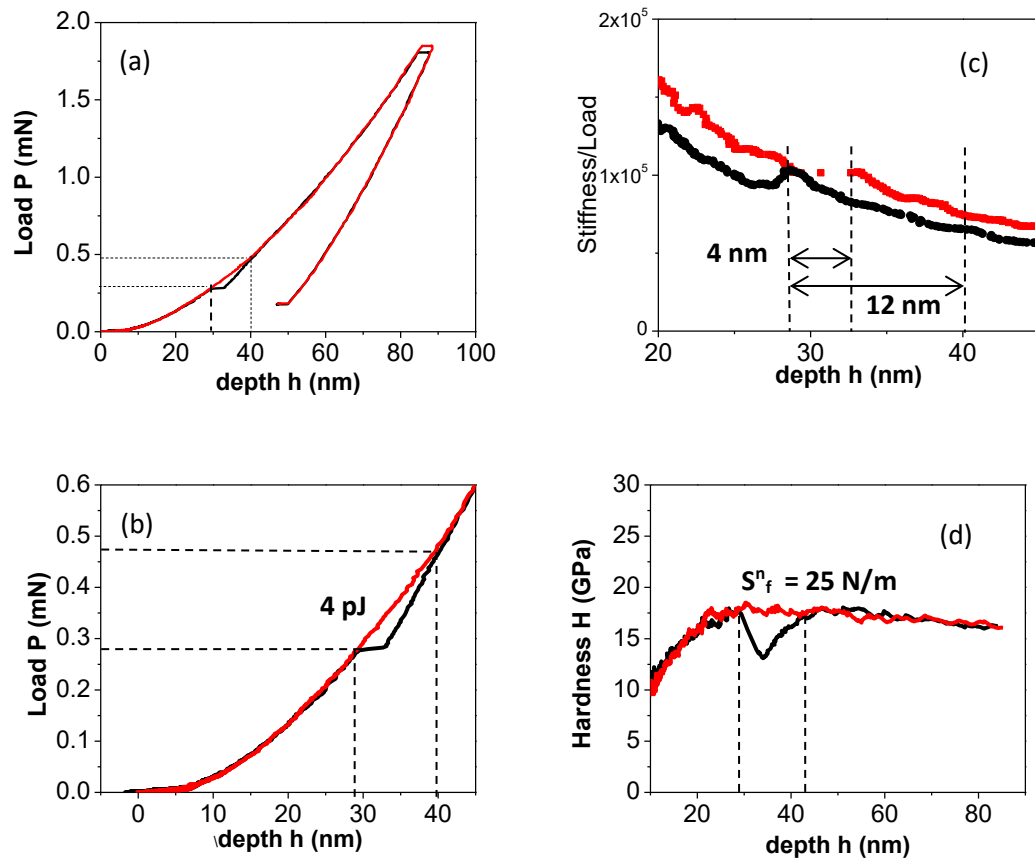


Fig 1(a) Load-depth (P - h) plots for fracture and no fracture cases and (b) its magnified view (c) Stiffness/Load vs depth of penetration (d) hardness profile for the two cases

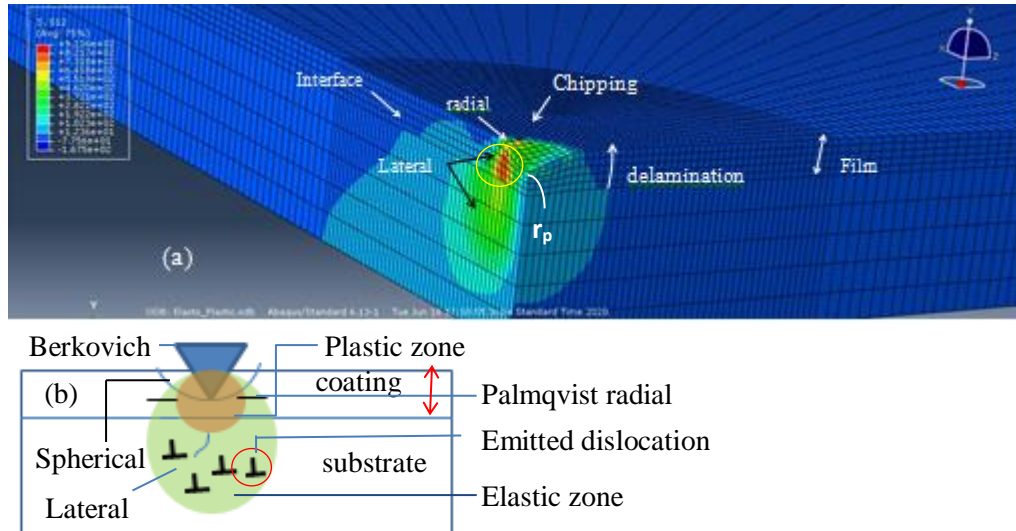


Fig 2(a) Finite Element modeling for nanoindentation carried out in a coating/substrate system
[10] (b) plastic and elastic zones due to tip blunting